How cockatiels (*Nymphicus hollandicus*) modulate pectoralis power output across flight speeds

Tyson L. Hedrick[1],*, Bret W. Tobalske[2] and Andrew A. Biewener[1]

[1]*Concord Field Station, Museum of Comparative Zoology, Harvard University, Old Causeway Road, Bedford, MA 01730, USA* and [2]*Department of Biology, University of Portland, 5000 N. Willamette Boulevard, Portland, OR 97203, USA*

*Author for correspondence (e-mail: thedrick@oeb.harvard.edu)

Summary

The avian pectoralis muscle must produce a varying mechanical power output to achieve flight across a range of speeds (1–13 m s^{-1}). We used the natural variation in the power requirements with flight speed to investigate the mechanisms employed by cockatiels (*Nymphicus hollandicus*) to modulate muscle power output. We found that pectoralis contractile function in cockatiels was generally conserved across speed and over a wide range of aerodynamic power requirements. Despite the 2-fold range of variation in muscle power output, many aspects of muscle performance varied little: duration of muscle shortening was invariant, and overall wingbeat frequency and muscle strain varied to a lesser degree (1.2-fold and 1.4-fold, respectively) than muscle power or work. Power output was primarily modulated by muscle force (accounting for 65% of the variation) rather than by muscle strain, cycle frequency or changes in the timing of force production relative to muscle strain. Strain rate and electromyogram (EMG) results suggest that the additional force was provided *via* increasing pectoralis recruitment. Due to their effect on the transformation of muscle work into useful aerodynamic work, changes in wing position and orientation during the downstroke probably also affect the magnitude of muscle force developed for a given level of motor recruitment. Analysis of the variation in muscle force and airflow over the wing suggests that the coefficients of lift and drag of the wing vary 4-fold over the speed range examined in this study.

Key words: cockatiel, *Nymphicus hollandicus*, flight, muscle, power.

Introduction

The goal of this paper is to investigate the underlying mechanism(s) by which birds modulate the mechanical power output of their pectoralis muscle in relation to changing aerodynamic power requirements associated with varying flight speed. Because of its size and central role in wing depression and lift production, the pectoralis muscle produces most of the mechanical power required for steady flight (Rosser and George, 1986; Dial, 1992; Dial and Biewener, 1993; Biewener et al., 1998). The production of mechanical power is of central importance to various modes of locomotion, including swimming, flying and acceleration or climbing in a terrestrial environment (McMahon, 1984; Vogel, 1994). However, the mechanisms that animals use to modulate power, including variation in muscle force (or stress), length change (or strain), cycle frequency and the timing of force production within the shortening cycle, are not well understood. These muscle properties are not mutually independent. Because of force–velocity effects, it is likely that trade-offs exist between the speed of muscle shortening and muscle force, as well as between shortening amplitude and contractile frequency (McMahon, 1984). Here, we investigate the importance of these general factors and their interaction over a wide range of usage *in vivo*. Several recent studies *in vitro* and *in vivo* have also examined factors that influence muscle power output, but these studies focus on maximal power activities (e.g. Askew et al., 2001; Coughlin, 2000; Josephson et al., 2000; Williamson et al., 2001) rather than a broad spectrum of function, such as bird flight over a range of speed.

Two broad strategies can be used to modulate muscle power output in cyclical locomotor modes such as avian flight. Muscle power output could be modulated by changes in wingbeat and muscle contraction frequency (strategy 1) or changes in the amount of work performed per cycle (strategy 2). Pectoralis work per cycle can, in turn, be modulated by changes in the strain amplitude experienced by the muscle (strategy 2A), changes in the amount of force produced by the muscle (strategy 2B) or other details of the contraction cycle that influence the force–strain trajectory such as the percentage of the cycle spent shortening, the timing of force production relative to strain or the specific strain trajectory (strategy 2C; Askew and Marsh, 2001). A previous study of pigeons (*Columba livia*) found that, over a broad range of flight

performance ranging from descending and level flight to take-off and vertical climbing flight, pectoralis force only varied by about 40%, much less than the >2-fold overall variation in power output (Dial and Biewener, 1993). The muscle's force–strain trajectory was also found to vary little over the range of flight conditions studied. Consequently, we hypothesized that modulation of muscle strain (strategy 2A) would be the primary source of variation in power output, with secondary contributions from modulation of muscle force (strategy 2B) and wingbeat frequency (strategy 1).

In support of strategy 2A, Williamson et al. (2001) found that differences in pectoralis power output during take-off *versus* slow level flight in mallard ducks (*Anas platyrhynchos*) were modulated mainly by means of variation in muscle strain. Warrick et al. (2001) also observed significant variation in muscle strain (1.3-fold) in the pectoralis of magpies (*Pica hudsonia)* associated with the modulation of power output across flight speeds. In their study of pectoralis power output across different flight modes and during load carrying in pigeons, Dial and Biewener (1993) found that muscle force varied 1.4-fold whereas muscle strain was estimated from kinematics to vary 1.3-fold. Hence, both factors contributed similarly to the 2.3-fold variation in power output, suggesting that birds may employ a combination of strategies 2A and 2B (strain and force) to modulate work and power output as a function of flight speed. Shifts in the timing of muscle force production with respect to muscle strain, included here as strategy 2C, were found to mediate the shift from minimal muscle power production in level running in turkeys (*Meleagris gallopavo*) to positive power production in uphill running (Roberts et al., 1997). However, flying birds must always produce positive power and may optimize the timing of muscle force *versus* muscle strain for power production at all speeds. Finally, although the vortex theory of avian flight (Rayner, 1979a,b) assumes that wingbeat frequency is fixed for a given species, it necessarily suggests that a change in frequency would have a strong influence on aerodynamic power output. As certain bird species are known to vary wingbeat frequency moderately with speed (1.2-fold; Tobalske, 1995), it is likely that some combination of the strategies described above is used to modulate power output during flight.

In this study, we measured *in vivo* pectoralis power output in cockatiels flying across a wide range of speeds in a wind tunnel and examined the variation in power due to the four different strategies described above. We also combined our muscle power analysis *in vivo* with a high-speed, three-dimensional (3-D) kinematic analysis to investigate how the observed changes in muscle power were applied to the environment *via* the wings.

Materials and methods

The materials and methods employed in this study generally follow those used in Tobalske et al. (2003) but are more completely described here.

Animals and flight training

Five cockatiels (*Nymphicus hollandicus* Kerr; 78.5±5.0 g, mean body mass ± S.D.) were purchased from a local licensed animal vendor and housed in a 1.7 m×2.7 m×3.3 m indoor aviary at the Concord Field Station animal care facility (Bedford, MA, USA), where they were provided with food and water *ad libitum*. The birds were trained to fly over a range of speeds from 1 m s^{-1} to 15 m s^{-1} in the Concord Field Station wind tunnel (Hedrick et al., 2002). Training lasted one month, comprising a minimum of five 30-min bouts of flight training per week. All individuals tended to fly in the upper forward quadrant of the working section of the wind tunnel. Cockatiels learned to fly at a steady speed in the wind tunnel in 2–4 days and were then exercised for at least three additional weeks to expand the speed range over which they would fly steadily prior to data recording. The trained cockatiels were willing to fly for at least 10 min without rest at 9 m s^{-1}. At very fast (>13 m s^{-1}) and slow (<3 m s^{-1}) speeds, the duration of flights that the birds were willing to sustain was typically ≤1 min. The maximum speed of each bird was defined as the highest speed at which it would voluntarily maintain its position in the wind tunnel for 30 s. All training and experimental procedures were approved by the Harvard University Institutional Animal Care and Use Committee.

Surgical procedures

Following training, the birds were anesthetized using isoflurane administered *via* a mask in order to implant sterilized sonomicrometry muscle length transducers, electromyography (EMG) electrodes and a deltopectoral crest (DPC) bone strain gauge. Once an appropriate plane of anesthesia was achieved, the feathers over the left shoulder, upper back and left mid-anterior region of the pectoralis were removed and the skin surfaces disinfected with betadine solution. A 2-cm incision was made over the ventral surface of the pectoralis and a 1-cm opening was made in the skin over the animal's back. These allowed the EMG and sonomicrometry crystal electrodes to be passed subcutaneously through the axilla and beneath the wing to the opening over the pectoralis. One pair of 1-mm sonomicrometry crystals (Sonometrics, Inc., London, Ontario, Canada) and a bipolar EMG electrode were then implanted parallel to the fascicle axis of the mid-anterior region of the sternobrachial (SB) portion of the pectoralis (Fig. 1A). In this region, the fascicles originate from the keel of the sternum and pass directly to the muscle's insertion on the ventral surface of the DPC of the humerus.

The avian pectoralis is well suited for making *in vivo* measurements of fascicle length change by means of sonomicrometry because of the parallel organization of the muscle's fibers at its superficial surface. In all birds, the sonomicrometry crystals were implanted at a depth of appoximately 4 mm beneath the superficial fascia of the muscle and at a distance of 8–12 mm apart. Small openings parallel to the fascicles were made by puncturing the surface of the muscle and spreading with small, pointed scissors. After inserting each sonomicrometry crystal and aligning them to
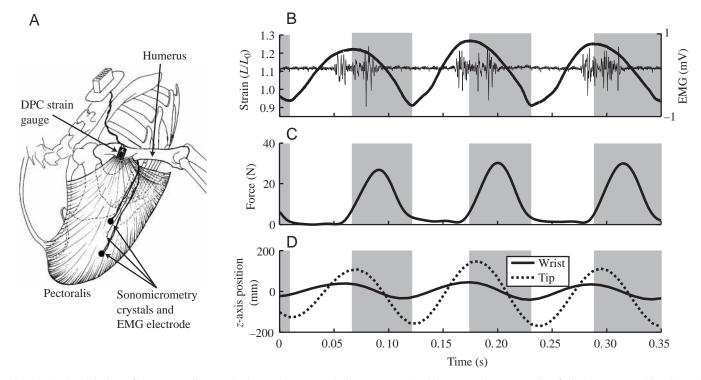
Fig. 1. (A) A depiction of the pectoralis muscle, its attachment to the humerus at the deltopectoral crest (DPC) of the humerus, and implanted transducers. A pair of sonomicrometry crystals was implanted in the proximal portion of the pectoralis, and an EMG electrode was placed between the two crystals. A metal-foil strain gauge was attached to the dorsal surface of the DPC of the humerus. Wires from all these transducers were passed subcutaneously to a customized miniature plug attached to the bird's back. (B) Sonomicrometry and electromyogram (EMG) recordings are shown for three successive wingbeats at 7 m s^{-1}. The time course of pectoralis shortening (downstroke) is shaded in gray. (C) Pectoralis force recorded by the strain gauge and (D) *z*-axis (vertical) motion of the wrist and wing-tip obtained from a 3-D reconstruction of digitized markers based on 125 Hz dorsal and lateral camera views.

ensure a maximum signal quality, these openings were sutured closed with 6-0 silk. A 4-0 silk suture was used to tie down the sonomicrometry lead wires a few millimetres away from the implantation site for strain relief and to eliminate movement artefact in the recorded signals. A fine-wire bipolar silver hook EMG electrode (0.5-mm bared tips with 2-mm spacing; California Fine Wire, Inc., Grover Beach, CA, USA) was implanted immediately adjacent to the sonomicrometry crystals to confirm that length change recordings represented activated muscle fibers. The EMG electrode was inserted at a shallow angle parallel to the fascicle axis using a 23-gauge hypodermic needle and anchored by a 6-0 silk suture at the exit point from the muscle's surface. A second tie was also made further back, close to the keel of the sternum, with a small loop of wire between the two ties that served as strain relief and helped to reduce movement artefact in the EMG signal.

Sonomicrometry

Sonomicrometry provides a direct measurement of muscle fascicle length change by recording the transit time of a series of ultrasonic sound pulses that are emitted by one crystal and received by the other of a pair. Use of the Triton 120.2 sonomicrometry system (Triton Technology Inc., San Diego, USA) requires a positive 2.7% correction to account for faster

speed of sound transmission in skeletal muscle (1540 m s^{-1}; Goldman and Hueter, 1956) and an offset adjustment of +0.16 mm for the faster sound movement through the epoxy lens of the 1.0 mm crystals, as well as a 5 ms correction for the phase delay introduced by the amplifier's filter. We verified the 5 ms phase delay using a signal generator and oscilloscope. Measurements of length change (Δl) are made between the two crystals; the resting length of the muscle fascicles (L_{rest}) was defined as the length that was recorded at the end of the flight sequence, after the bird had landed on the perch and remained at rest with its wings held at its sides. This was also verified by obtaining post-mortem length recordings. Fractional length change, or fascicle strain (ε), was determined as $\varepsilon = \Delta l / L_{rest}$. To calculate muscle work and muscle power, total fascicle length change (ΔL) was calculated as $\Delta L = \varepsilon L_0$ (where L_0 is the resting length of the entire fascicle along which the crystals were implanted). Measurements of ΔL therefore assume uniform length change along the entire length of the fascicle. Following the completion of the experimental recordings, we performed a post-mortem dissection to verify the alignment of the sonomicrometry crystal implants with respect to the fascicle axis using a protractor. In all cases, the crystals were found to be well-aligned ($\pm 2°$ with the muscle fascicle axis, rendering alignment errors of muscle length change insignificant).

DPC strain recordings of muscle force

In addition to implanting sonomicrometry and EMG electrodes within the pectoralis, we also attached a single element metal-foil strain gauge (FLE-1, Tokyo Sokki Kenkyujo, Ltd, Tokyo, Japan) to the dorsal surface of the deltopectoral crest (DPC) of the cockatiel humerus (Fig. 1A). This was done by making a small (10 mm) incision over the left shoulder and reflecting the overlying deltoid muscle to expose the bony surface of the DPC. The strain gauge and its lead wires were passed subcutaneously and deep to the deltoid muscle to the DPC installation site. After lightly scraping the overlying periosteum with a scalpel and drying the bone surface with a cotton applicator dipped in methyl-ethyl-ketone, the strain gauge was bonded to the dorsal surface of the DPC, perpendicular to the humeral shaft, using a self-catalyzing cyanoacrylate adhesive. Strain recordings obtained from the DPC were used to quantify pectoralis force generation under *in vivo* flight conditions (see below). During the downstroke, the DPC is pulled ventrally by the contracting pectoralis, so that the dorsal surface develops a principal axis of tensile strain that is nearly perpendicular to the long axis of the humerus (Dial and Biewener, 1993). This makes the strain gauge sensitive to forces produced by the pectoralis but not to other muscle or aerodynamic forces transmitted by the bone between the elbow and the shoulder.

Following implantation of the DPC strain gauge and the muscle electrodes, all of the wounds were sutured closed. A customized miniature back plug, previously soldered to the transducers' lead wires and insulated prior to surgery, was anchored to the skin and vertebral ligaments using 3-0 silk. The animals were then allowed to recover for 24 h prior to making experimental recordings in the wind tunnel.

Flight recordings

Experimental recordings of pectoralis EMG, fascicle length change and DPC strain were made during the following day. These recordings were made by connecting the animal to a lightweight multi-lead cable that ran a distance of 1 m from the back connector on the animal to a small (0.75 cm diameter) opening at the top of the wind tunnel's working section. The combined mass of the data cable section within the wind tunnel and the back plug was 12.8 g, or 15% of the animal's body mass. This lightweight cable connected to a heavier, shielded cable that ran to the recording amplifiers (Micromeasurements Vishay 2120 strain gauge bridge amplifier; Grass P-511 EMG amplifier; and Triton 120.2 sonomicrometry amplifier). The outputs of each of these amplifiers were sampled by an A/D converter (Axoscope Digidata 1200) at 5 kHz and stored on a computer for subsequent analysis. Muscle strain and force recordings were subsequently filtered with a 50 Hz digital Butterworth low-pass filter to remove high-frequency noise; EMG recordings were filtered with a 250 Hz digital Butterworth high-pass filter to remove low-frequency artefacts. Recordings were obtained over a range of speeds for each animal (1 m s^{-1}, 3 m s^{-1}, 5 m s^{-1}, 7 m s^{-1}, 9 m s^{-1}, 11 m s^{-1} and 13 m s^{-1}). Although the cockatiels were trained to fly at speeds of up to 15 m s^{-1} in the wind tunnel, none of the individuals were able to attain this speed following surgery and with the additional drag of the data cable and plug.

Wind tunnel

The Concord Field Station wind tunnel is an open-circuit tunnel with a closed flight chamber (Hedrick et al., 2002). Briefly, it has a working section 1.2 m×1.2 m in cross-section and 1.4 m in length and can operate at wind speeds from 0 m s^{-1} to 28.5 m s^{-1}. Average variation in mean flow velocity within the working section is 1.03%, and average turbulence is 1.10%. In order to make our measurements, obtained under the atmospheric conditions of the tunnel's location in Bedford, MA, USA (58 m above sea level; mean air temperature during data collection was 26.1°C, and air pressure was 100.6 kPa), comparable with measurements obtained from studies involving wind tunnels at other locations, we followed Pennycuick et al. (1997) in reporting equivalent wind speed (V_e) rather than true wind speed:

$$V_e = \sqrt{2q/\rho_0}\,, \qquad (1)$$

where q is the dynamic pressure ($0.5\rho u^2$), ρ_0 is air density at sea level (1.225 kg m^{-3}) and u is wind speed.

Video recording and 3-D coordinate reconstruction

Flight trials were recorded using two synchronized, high-speed digital video cameras (Redlake PCI 500) operating at 250 frames s^{-1} or 125 frames s^{-1} with a shutter speed of 1/1250th of a second. The lower recording frequency was used for later trials in order to double the recording duration to facilitate analysis of a greater number of wing beats, as it was not found to have a significant effect on our kinematic analyses (see below). One camera was placed lateral to the flight chamber and the other above and behind it. The camera data were synchronized with the sonomicrometry, strain gauge and EMG data by recording the camera's digital trigger together with the muscle signals *via* the A/D converter. The cameras were calibrated using the modified direct linear transformation (DLT) technique with a 54-point calibration frame (measuring 0.624 m×0.900 m×0.700 m in *xyz* coordinate space) that was recorded at the end of each set of trials (Hatze, 1988). Trials were recorded at flight speeds of 1–13 m s^{-1} in 2 m s^{-1} intervals. Flight speed sequence was not restricted to a particular order and the birds were allowed to rest between trials as necessary to maintain satisfactory performance (typically 2–5 min of steady flight).

Three points (dorsal and ventral surfaces of the shoulder, wrist and tip of the ninth primary) were identified on the right wing of each bird using 5-mm-diameter circles of white tape marked with a black center dot. In addition, markers were placed on the back plug where it attached to the dorsal midline between the wings and at the base of the tail. Flight sequences consisting of a minimum of three successive wingbeats with minimal lateral and vertical movement within the flight chamber (within-chamber speed <0.3 m s^{-1}) were selected

from the video data and digitized using custom software written in Matlab v.5.3 (The MathWorks, Natick, MA, USA). In the few cases where sequential wingbeats with minimal change in wind tunnel position were not available, we selected additional wingbeats from the recorded flight sequence, digitizing at least three wingbeats for each individual at each speed. In trials that were recorded at 250 Hz, we digitized every other frame, resulting in an effective video recording frequency of 125 Hz for all trials.

The raw coordinate data obtained from the digitized trials were resolved into a single 3-D space using the DLT coefficients derived from the calibration frame (Hatze, 1988). In addition to resolving the dorsal and lateral 2-D camera views into a single 3-D space, the DLT method also corrects for parallax and other lens distortions. Individual points having a DLT root mean square error (rms error) two standard deviations greater than the median rms error for that point (approximately 4% of the points) were removed prior to analysis. Median rms error ranged from 1.84 mm for the shoulder marker to 6.62 mm for the ninth primary tip. Occasionally, a point was not in the view of both cameras, resulting in a gap in the reconstructed point sequence; this occurred in approximately 5% of the points digitized. All points were filtered, and missing or dropped points were interpolated with a quintic spline fit to known rms using the Generalized Cross Validatory/Spline (GCVSPL) program (Woltring, 1986). This method uses the rms from the DLT reconstruction to filter the positional data and then fills any gaps with a quintic spline interpolation. The results from this technique were similar to those obtained by smoothing the positional data using a 37 Hz digital Butterworth low-pass filter. However, the quintic spline method also allows direct calculation of velocity and acceleration derivatives from the spline curves, providing the most accurate method for obtaining higher order derivatives from positional data (Walker, 1998).

Morphological measurements

After experimental recordings were completed, the animals were euthanized by an overdose of sodium pentobarbitol

Table 1. *Morphometric data for the cockatiel (*Nymphicus hollandicus*) and experimental conditions*

Variable	Mean ± S.D.
Body mass (g)	83.0±5.0
Total pectoralis mass (g)	16.9±0.6
Fascicle length (mm)	34.9±5.0
Wing span (mm)	463.0±31.0
Wing chord (mm)	70.2±3.0
Air temperature (°C)	26.4±1.7
Air pressure (kPa)	100.6±0.3
Air density (kg m^{-3})	1.17±0.01

N=5 in all cases. Measurements were made with the wings spread as in mid-downstroke.

(100 mg kg^{-1}, i.v.) in order to obtain morphometric measurements. These included pectoralis mass, fascicle length and pinnation angle, wingspan and mean wing chord (Table 1).

Aerodynamic power analysis and muscle power calibration

Aerodynamic power (P_{aero}) produced by the pectoralis muscle was estimated on a per-wingbeat basis from the 3-D kinematic reconstruction by summing separate estimates of induced (P_{ind}), profile (P_{pro}), parasite (P_{par}) and climb power (dE_p/dt, where E_p is potential energy and t is time) for each video frame then integrating over a complete wingbeat cycle (typically 13–18 frames):

$$P_{aero} = P_{par} + P_{ind} + P_{pro} + \frac{dE_p}{dt} . \qquad (2)$$

Parasite power was estimated by:

$$P_{par} = \tfrac{1}{2}\rho C_{D,par} V_t^3 \qquad (3)$$

(Rayner, 1979a,b), where ρ is air density, V_t is the sum of effective air velocity in the tunnel working section and any forward or rearward motion of the bird, and $C_{D,par}$ is the parasite drag coefficient, which was estimated according to Rayner (1979a; equations 17 and 20). We added the power required to overcome drag from the data cable to P_{par}. Drag from the cable was measured by attaching the cable to a piezoelectric load cell (Kistler 9203) placed in the wind tunnel, with the cable positioned above the load cell to its exit point from the working section to simulate its position above the bird in flight.

We estimated induced power as:

$$P_{ind} = \frac{T^3}{(2\rho A_0)^2} \ k_{ind} , \qquad (4)$$

where T is thrust, A_0 is actuator disc area, and k_{ind} is the induced power correction factor (Wakeling and Ellington, 1997). A_0 was calculated by:

$$A_0 = \phi R^2 \cos\theta , \qquad (5)$$

where ϕ is wing stroke amplitude, R is wing length, and θ is the angle of the stroke plane relative to vertical. We used an induced power correction factor, k_{ind}, of 1.2 (Pennycuick, 1975). We calculated the thrust required as:

$$T = - M_b \mathbf{g} + M_b \ddot{\mathbf{z}} - \frac{P_{par}}{V_t} \qquad (6)$$

(Wakeling and Ellington, 1997), where $\mathbf{g}$ is acceleration due to gravity, M_b is body mass and $\ddot{\mathbf{z}}$ is vertical acceleration of the bird as measured by the 2nd derivative of a quintic spline fit to the z-axis position of the dorsal marker on the bird.

Profile power was estimated by:

$$P_{pro} = 2 \sum_{i=1}^{25} \tfrac{1}{2}\rho V_i^3 C_{D,pro} a_i , \qquad (7)$$

where V_i is the total velocity (including velocity due to flapping) of wing section i, $C_{D,pro}$ is the profile drag coefficient, assumed to be 0.02, and a_i is the area of the wing section (Rayner, 1979a,b; Norberg, 1990).

After estimating the aerodynamic power requirement for a given wingbeat, we compared this value to the uncalibrated muscle power for that wingbeat and calculated the correction factor, F, necessary to make uncalibrated muscle power equal to aerodynamic power. Because the only unknown in the conversion from uncalibrated to calibrated muscle power is a constant term converting strain gauge voltage to newtons, F is the strain gauge calibration constant. For each bird, we calculated a mean F from at least five wingbeats at flight speeds of 7 m s^{-1} and 9 m s^{-1} and used this mean F to calibrate muscle power for all wingbeats at all speeds for that individual. We used these speeds to calculate F because the assumptions employed in the aerodynamic power calculation are most reasonable at intermediate flight speeds. The mean coefficient of variation (CV) of F was 12.5±5.0% within individuals. All calculations were performed in Matlab v.5.3.

We adjusted the strain gauge calibration constant using the aerodynamic power method as described above rather than using the direct 'pull' calibration method we have used in the past (Biewener et al., 1992, 1998; Dial and Biewener, 1993). We adopted this approach because we found our previous method to be unreliable owing to the difficulty of accurately representing the *in vivo* transmission of tensile force by the pectoralis to the base of the DPC in this and another (ringed turtle-dove, *Streptopelia risoria*) species. Repeated pull calibrations performed on the cockatiels had a mean CV of 24.5±11.0% among individuals. By directly pulling along the superficial surface of the muscle beneath its insertion site, force transmission is likely biased to the more distal region of the DPC. To the extent that this occurs, this will increase the bending moment applied to the DPC and result in an underestimate of strain-calibrated force. In addition, this calibration method can give varying force–strain slopes for differing cranio-caudal orientations of pull, which may also be problematic given the varying orientation with which the pectoralis can pull on the DPC due to its own fiber architecture and the changing elevation and depression of the humerus during the wingbeat cycle.

We evaluated the accuracy of the aerodynamic power calculated from 250 Hz *versus* 125 Hz video data by digitizing results at several speeds at 250 Hz, calculating the aerodynamic power, then reducing the data to 125 Hz by selecting every other point and re-calculating the aerodynamic power. In each case, the aerodynamic power estimates for the two different recording frequencies were within 5% of one another and not significantly different [analysis of variance (ANOVA), d.f.=13, P=0.72]. Consequently, we concluded that a 125 Hz video acquisition frequency was sufficient for this study. We also examined the influence of our aerodynamic assumptions on F by recalculating the aerodynamic power results using alternative 'low-power' and 'high-power' values of k_{ind}, $C_{D,pro}$ and $C_{D,par}$. In the low-power case, k_{ind} was decreased from 1.2 to 1.0, and $C_{D,par}$ and $C_{D,pro}$ were decreased by 50% to 0.065 and 0.01, respectively; for the high-power case, k_{ind} was increased to 1.4, and $C_{D,par}$ and $C_{D,pro}$ were increased by 50% to 0.195 and 0.03, respectively. This allowed us to bracket the likely range of pectoralis power that might be observed at any particular flight speed. Had we used the 'pull' calibration technique in this study, the power output results would have been similar in magnitude to the low-power aerodynamic calibration but would have exhibited greater inter-individual variation. Finally, although the calibration factor F is necessary for calculating the magnitude of muscle power output, it does not affect the percentage variation in power across speeds with respect to the mean power. This makes our analysis of the factors contributing to variation in power output insensitive to differences in the value of F.

Potential effects of wind tunnels on bird flight performance

Conditions within a wind tunnel undoubtedly affect bird flight performance (Rayner, 1994). The unusual surroundings, noise and lights have unknown effects upon performance, and we tried to minimize these effects with adequate acclimation and training of the birds. Additionally, the wake of the bird may circulate within the flight chamber, reflect off the walls of the closed-section flight chamber and interact with the bound circulation on the wings. Due to this phenomenon, flight speeds and mechanical power requirements are expected to be less in a closed flight chamber compared with free flight without ground effect (Rayner, 1994). The effects of wake reflection are expected to decrease with increasing flight speed. Wind-tunnel effects are well documented for fixed-wing models (Barlow et al., 1999) but not for birds engaged in flapping flight. One study that compares wind tunnel and free flight performance in a bird suggests that mean wingbeat frequency is lower in the field, and other wing kinematics exhibit slight differences between tunnel and free flight (Tobalske et al., 1997).

Aerodynamic corrections for bird flight in a closed-section wind tunnel take into account the ratio of the diameter of the flight chamber to the wingspan and also the position of the bird inside the chamber. The chamber diameter:wing-span ratio was 2.48 for the cockatiels, and they generally flew near the horizontal mid-plane or slightly above. This position equates to h/H values that ranged from 0 to 0.25, where h is altitude of the body above the midline of the flight chamber, and H is vertical height of the flight chamber (Rayner, 1994). Using Rayner's (1994) model, for these animal dimensions and positions, minimum power and maximum range speeds may have been reduced by 3%, and mechanical power at these speeds may have been reduced by up to 10% relative to the same speeds in free flight. Given the uncertain nature of these adjustments, we do not make any corrections for wind tunnel effects in the results we report.

Statistical analysis

Comparisons across individuals and speed were performed using repeated-measures ANOVA. Least squares and multiple

regression statistics were used to examine the effect and importance of different factors both within and among individuals and speeds. In cases where we examined a series of sequential wingbeats, we tested for serial autocorrelation using Durbin's *h* test (Durbin, 1970). When autocorrelation was detected ($P \leq 0.05$), we removed it by sampling every other wingbeat from the original data set, which reduced *h* to acceptable levels in each case. We also employed Fisher's protected least-significant difference (PLSD) in certain pairwise comparisons and used a path analysis to place the multiple regression results in the context of a general model for muscle power output (Sokal and Rohlf, 1995). Statistical analysis was performed using Stata 6.0 (Stata Corporation, College Station, TX, USA); *P* values of ≤ 0.05 were used to denote significance. We report means ± S.D. among individuals, which were obtained from a minimum of 17 and a mean of 46 wingbeats per individual per flight speed.

Results

In vivo *patterns of pectoralis force, length change and neural activation*

We found that the cockatiel pectoralis underwent large strains (0.39±0.03; range, 0.34–0.44) and developed forces of up to 39 N (29.5±6.0) during contraction over a range of flight speeds. Although the general features of the contraction cycle (Figs 1B, 2, 3) are consistent from wingbeat to wingbeat and across speeds, the precise timing of the events varied among successive wingbeats at the same flight speed and among speeds. EMG activation preceded the onset of muscle force production by an average of 7.8±1.1 ms and did not vary significantly with speed (Figs 1, 2; Table 2). Activation preceded the start of muscle shortening by an average of 13.2±2.4 ms. This lag varied by a factor of 1.7 over the speed
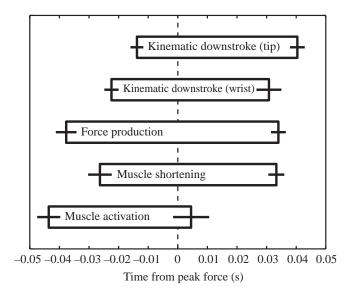

Fig. 2. A timing histogram relating the timing of electromyogram (EMG) activity, muscle length change, muscle force production and kinematic data for an individual bird flying at 7 m s⁻¹. The zero time is set to the time at which maximum force occurred, which corresponds to mid-downstroke. The bars on each rectangle indicate standard deviation. Additional data on the variation across speeds in the relationship between EMG onset time, muscle shortening and force production are given in Table 2.

range studied, becoming slightly greater and more variable at higher flight speeds (Table 2). Muscle activation typically continued until slightly before or after the muscle reached maximum force (Fig. 2). Activation duration averaged 54.0±6.1 ms and did not vary significantly with speed (Table 2). Muscle shortening and force production ended simultaneously at all flight speeds.
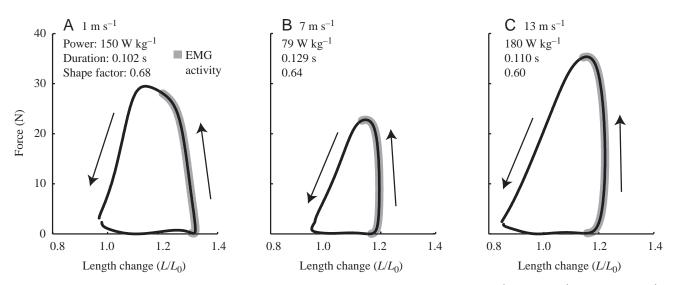

Fig. 3. Whole wingbeat *in vivo* work loops obtained from an individual cockatiel flying at (A) 1 m s⁻¹, (B) 7 m s⁻¹ and (C) 13 m s⁻¹. The direction of each loop is counter-clockwise, resulting in positive work. Pectoralis mass-specific power output, wingbeat duration and work 'shape factor' are noted in the upper left for each loop. The shape factor quantifies work loop shape by dividing the actual loop area by the theoretical maximum area for the observed peak force and length change.

Table 2. *Muscle power output and associated subcomponents during the flapping flight of the cockatiel (Nymphicus hollandicus)*

Variable	Flight speed (m s⁻¹)							F	P
	1	3	5	7	9	11	13		
Mass-specific pectoralis power output (W kg⁻¹)	125.1±24.1	96.1±21.9	73.5±10.1	76.9±11.3	96.6±22.5	118.1±23.4	155.6±29.2	6.308	0.0004*
Positive work per wingbeat (J)	0.23±0.04	0.18±0.04	0.14±0.02	0.16±0.02	0.21±0.03	0.26±0.04	0.32±0.05	6.972	0.0002*
Total pectoralis length change (L)	0.41±0.06	0.38±0.04	0.34±0.05	0.36±0.08	0.39±0.08	0.42±0.05	0.44±0.06	7.308	0.0002*
Peak pectoralis force (N)	31.8±9.1	27.0±8.2	22.3±5.2	23.3±4.2	28.3±4.5	34.6±5.3	38.9±4.9	7.544	0.0001*
Wingbeat duration (ms)	109.0±6.0	118.1±8.4	119.5±3.8	130.9±6.4	133.9±8.6	135.0±7.8	122.5±5.8	7.927	0.0001*
Downstroke duration (ms)	67.2±2.5	70.2±4.2	66.6±3.1	66.9±4.3	67.7±6.8	67.4±5.2	66.1±3.9	0.821	0.5645
Upstroke duration (ms)†	41.8±4.0	47.9±6.3	52.9±3.2	64.0±4.6	66.3±4.2	67.5±6.6	56.4±6.1	14.18	0.0001*
EMG duration (ms)†	48.1±7.9	50.3±8.7	54.5±12.6	59.5±19.8	61.7±17.9	57.4±8.6	50.2±4.4	1.72	0.2624
EMG onset to force production (ms)†	9.4±4.9	8.7±4.3	8.6±3.8	6.6±1.0	7.2±2.2	7.6±2.7	6.6±1.04	1.02	0.4888
EMG onset to pectoralis shortening (ms)†	10.7±1.4	9.7±1.3	12.4±1.5	15.2±3.1	16.0±4.2	14.7±4.6	13.9±4.7	5.45	0.0291
Work loop shape factor	0.52±0.08	0.53±0.06	0.55±0.06	0.56±0.06	0.55±0.05	0.53±0.05	0.54±0.05	1.01	0.4398
Pectoralis shortening velocity (L s⁻¹)	6.11±0.87	5.42±0.77	5.19±0.81	5.43±1.07	5.77±0.98	6.20±0.80	6.73±0.98	13.12	0.0001*

Values are inter-individual means ± s.d.; $N=5$ († indicates $N=2$).
Significant effects of flight speed at the $P<0.05$ level after a Bonferroni correction for the table are marked with an asterisk (repeated-measures ANOVA with individual and speed; d.f.=6).

Wing kinematics versus in vivo pectoralis length change

We found that kinematic measurements of downstroke initiation and duration differed from those obtained *via* sonomicrometry (Fig. 2). Both the wrist and wing-tip motion in the vertical axis lagged muscle shortening, with a greater lag at the end of the downstroke than at the start. The wing-tip had a noticeably greater lag (12.5±3.1 ms), possibly due to bending of the feathers at the beginning and end of the downstroke (Fig. 2). However, wrist motion also lagged muscle contraction by a small margin (3.9±3.2 ms). This lag is probably due to (1) long-axis rotation of the wing causing vertical movement of the wrist, (2) movement at the elbow joint and (3) the difficulty of precisely tracking the relatively small amplitude motions of the wrist. Although the difference between the sonomicrometer and video sampling frequencies (5000 Hz *versus* 125 Hz) could contribute to the observed lag between muscle shortening and kinematics, we found that video trials digitized at 250 Hz compared with 125 Hz had no observable effect on the lag between these variables. Use of wrist kinematics, rather than direct recordings of pectoralis shortening, therefore, results in a shorter estimate of downstroke duration (mean reduction for all flight speeds: 19%) and corresponding longer estimate of upstroke duration.

Pectoralis power output

We measured the pectoralis power output by dividing the muscle work performed in a wingbeat cycle by the cycle duration; *in vivo* mechanical work performed by the pectoralis during a wingbeat was quantified using the 'work loop' technique (Josephson, 1985). In most wingbeats, the work loops were wholly positive (Fig. 3). On occasion, a very small (<1.5% of the total area) negative work region of the loop occurred at the start of muscle shortening. However, only positive work contributes to aerodynamic power (Askew et al., 2001) and we based all further analyses of work on the positive component only. As previously reported (Tobalske et al., 2003), pectoralis power output varied 2.1-fold ($P<0.0001$) over the range of flight speeds examined in this study (Fig. 4A; Table 2) and was greatest at the slowest and fastest speeds tested (1 m s⁻¹ and 13 m s⁻¹). The cockatiels' minimum power speed flying in the wind tunnel was 5 m s⁻¹, and their maximum range speed or minimum cost of transport occurred at 9 m s⁻¹. The overall relationship between muscle mechanical power output and speed was generally U-shaped, similar to that predicted by aerodynamic theory. The relationship of power *versus* speed was similar for the individual birds studied (Fig. 4B). Variation in power output among sequential wingbeats within a bird at a given speed was generally large (mean CV=0.19) and was minimized at the intermediate speed of 5 m s⁻¹ (mean CV=0.13). We report power output as the mean of measurements obtained for ≥17 individual wingbeats of each bird flying at a given speed (Table 2).

Wingbeat frequency and pectoralis duty factor

Wingbeat duration varied significantly by a factor of 1.2 across the range of speeds studied (Fig. 5; Table 2). Maximum
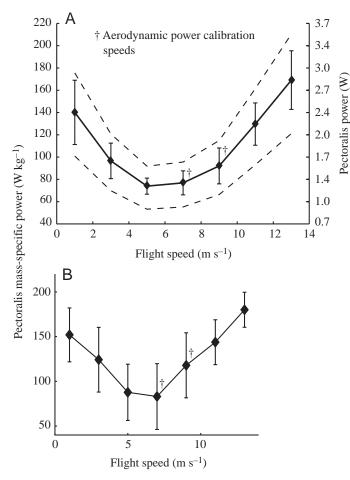
Fig. 4. (A) The relationship between mechanical power output and flight speed expressed as inter-individual means ± S.D. (*N*=5 for each speed; mean and minimum wingbeat sample sizes were 46 and 17, respectively, across all individuals). Pectoralis force recordings were calibrated using an aerodynamic power analysis at two intermediate flight speeds (7 m s^{-1} and 9 m s^{-1}). The broken lines indicate the possible range of variation in muscle power output given varying aerodynamic assumptions. (B) A power curve for an individual cockatiel showing within-individual means ± S.D. (mean and minimum sample sizes were 50 and 19 wingbeats, respectively, per animal for each speed). The cockatiels tended to repeatedly gain and lose potential energy while flying in the wind tunnel, leading to large variation in per-wingbeat power output at all but the fastest speeds. We restricted our analysis to sequences of wingbeats with no net change in potential energy but allowed individual wingbeats that resulted in a change in potential energy.
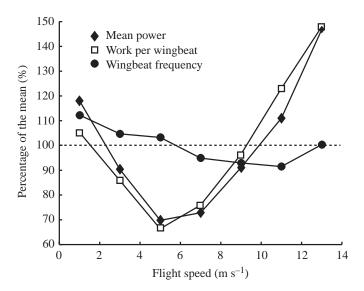

Fig. 5. Variation in pectoralis power, pectoralis work and wingbeat frequency across flight speeds. All values are inter-individual means (*N*=5 for each speed) normalized as a percentage of the overall mean for each parameter. Standard deviations are not shown to improve clarity (these are presented in Table 2). These data show that pectoralis power is determined mainly by changes in muscle work per wingbeat and not by wingbeat frequency.

duration of the two phases was approximately equal at intermediate speeds (7–11 m s^{-1}). We found similar overall patterns when we measured upstroke and downstroke *via* the vertical motion of the wrist in the 3-D kinematic reconstruction rather than muscle length change, but the relative durations of the phases differed between the two methods (Fig. 6). Downstroke duration measured kinematically was also constant across speeds but was shorter by an average of 12.9±3.1 m s^{-1} (13% of the wingbeat cycle) and upstroke was correspondingly longer. This shift was sufficient to make kinematic upstroke equal in duration to downstroke at slow speeds and fast speeds and much greater at intermediate speeds (Fig. 6B).

Although wingbeat frequency varied with flight speed, downstroke duration did not. Therefore, the duty cycle of the pectoralis, the percentage of the wingbeat cycle spent shortening, was not independent of wingbeat frequency. Pectoralis duty cycle varied from 61.5±3.2% of the cycle at 1 m s^{-1} to 49.6±2.9% at 11 m s^{-1}, following the same pattern of variation as wingbeat frequency (Fig. 6A). Because duty cycle was not independent of wingbeat frequency, we were unable to incorporate duty cycle into our component model of power output (see below). As a result, any effects due to the variation in duty cycle were included in the effect of wingbeat frequency, which accounted for only 10% of the variation in power output among speeds.

Pectoralis work

In addition to calculating the work loop areas, we quantified work loop shape by dividing the area within the loop by the

wingbeat duration occurred at a flight speed of 11 m s^{-1}, only slightly slower than the maximum speed the birds sustained in this study (13 m s^{-1}). Partitioning total wingbeat duration into muscle lengthening (upstroke) and muscle shortening (downstroke) phases (Fig. 6A) showed that shortening duration did not vary significantly across flight speeds. Thus, all variation in wingbeat duration was due to changes in muscle lengthening duration (Table 2). Lengthening duration was less than shortening duration at slow flight speeds (1–5 m s^{-1}) and at the fastest speed (13 m s^{-1}), whereas the

theoretical maximum (rectangular) area defined by the observed force and strain. This work loop 'shape factor' averaged 0.54±0.01 (i.e. 54±1% of the theoretical work space was achieved by the muscle's contraction). Interestingly, this did not vary significantly across speeds (Table 2). Pectoralis work per wingbeat varied significantly across the range of speeds by a factor of 2.3 (Fig. 5; Table 2). Pectoralis work reached a minimum at 5 m s^{-1}; the same speed at which power was minimized.

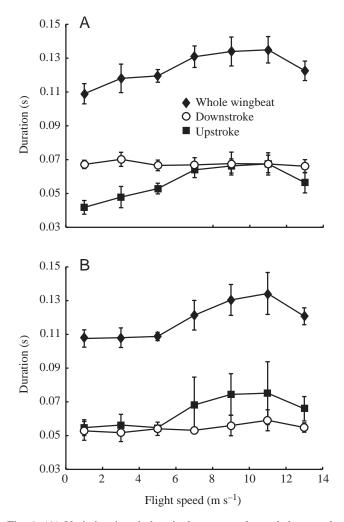Fig. 6. (A) Variation in whole wingbeat, upstroke and downstroke durations across flight speeds (inter-individual means ± S.D.; N=5 for each speed) as measured *via* muscle lengthening and shortening. Consistent with the modest change in wingbeat frequency *versus* speed (Fig. 5), wingbeat duration varies slightly but significantly (P<0.05; Table 2) with speed. Changes in wingbeat duration across speeds is due entirely to changes in upstroke duration, as downstroke duration does not vary significantly with speed (P>0.1; Table 2). (B) Variation in wingbeat duration measured *via* a 125 Hz, three-dimensional kinematic reconstruction. Although the general pattern is similar to that shown in A, the relative durations of upstroke and downstroke have shifted such that downstroke is shorter than or equal to, rather than longer than or equal to, upstroke.

Modulation of pectoralis force and length change as a function of speed

Whereas muscle power output is determined by muscle work in relation to wingbeat frequency, muscle work is determined by the particular pattern of force in relation to length change that a muscle develops. Although the particular work loop shape of a muscle cannot be explicitly defined in simple mathematical terms, patterns of peak muscle force and total muscle length change should be good predictors of the work performed by a muscle over a contractile cycle. Pectoralis force, length change and strain rate all varied significantly with speed, exhibiting minima and maxima at the same speeds as pectoralis power output (Fig. 7; Table 2). However, their respective ranges of variation were less than that of pectoralis work and power. Length change and peak force varied 1.4-fold and 1.7-fold, respectively, compared with a 2.3-fold variation in pectoralis work. Because downstroke duration did not vary with speed whereas muscle length change (strain) varied by a factor of 1.3, the rate of muscle shortening also varied 1.3-fold (Table 2).

A component model of pectoralis power output

We used a component model to quantify the variation in power output across flight speeds due to changes in wingbeat frequency, muscle length change, peak muscle force and work loop shape (Fig. 8). This path analysis indicates the strength of the relationship between components by showing the partial regression coefficients along the relationship lines. We found that approximately 90% of the variation in power output was attributable to variation in the work performed per wingbeat; the remaining portion was attributable to changes in wingbeat frequency. Work per wingbeat itself was most influenced by

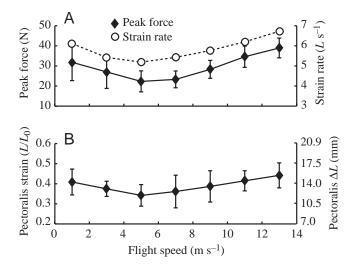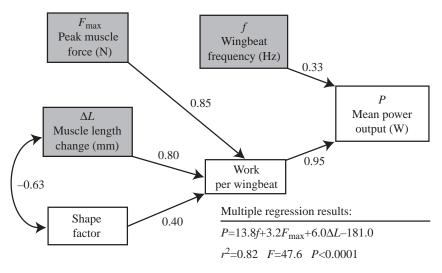Fig. 7. (A) Variation in peak muscle force and muscle strain rate as a function of flight speed. (B) Changes in the amplitude of muscle strain with speed (P<0.01; Table 2). Values represent inter-individual means ± S.D. (N=5 for each speed). Pectoralis force, strain rate and strain amplitude vary similarly with speed, and the pattern of variation matches that found for muscle power output *versus* speed (Fig. 5).

Fig. 8. A partial regression component model of the factors underlying pectoralis power output among individual birds as a function of flight speed with a least-squares multiple linear regression of power against selected factors. The arrows indicate the proposed relationships between variables, together with their partial regression coefficients, which indicate the relative strength of the relationship. Pectoralis power output as a function of flight speed is determined by the combination of work per wingbeat and wingbeat frequency, but work per wingbeat exerts the strongest effect. Pectoralis work per wingbeat is influenced by several factors, but the two most important are muscle force (r^2=0.77) and muscle length change (r^2=0.45; also see Fig. 6). The double-headed arrow between muscle length change and work loop shape factor indicates that increases in length change are correlated with decreases in the shape factor, and *vice versa*. The correlation also influences the total effect of the variables; for example, the total effect of muscle length change is 0.80–(0.63×0.40), or 0.55. There were no significant correlations between model variables aside from those indicated in the model *via* arrows. Statistical tests were conducted based on a set of individual means across speeds (5 individuals × 7 speeds: N=35).

Multiple regression results:

P=13.8f+3.2F_{max}+6.0ΔL–181.0

r^2=0.82 F=47.6 P<0.0001

the peak force developed during contraction, which accounted for approximately 70% of the variation in work and therefore 65% of the variation in power. Muscle length change accounted for approximately 20% of the variation in work. Changes in work loop shape accounted for the balance but were inversely related to muscle length change. The overall effect of increasing shape factor (increasing the realized fraction of ideal muscle work space), therefore, was to *reduce* the work performed per wingbeat. A multiple regression analysis of power output using the three most basic factors – wingbeat frequency, peak muscle force and muscle length change – was highly significant and had an r^2 of 0.82 (Fig. 8). In summary, peak muscle force was the best predictor of muscle work per wingbeat, which was the best predictor of power output. The relationship of these factors to the modulation of power output over successive wingbeats within any particular flight speed was more complex, with significant correlations observed between various performance components of the model (Table 3). Nevertheless, peak muscle force remained the dominant factor.

Muscle recruitment in relation to force and shortening velocity

For the two cockatiels in which high-quality EMG signals were recorded, we found that pectoralis EMG mean spike amplitude (measured as rectified area divided by duration) was a good predictor of muscle force, and therefore of pectoralis power output, across a range of flight speeds (Fig. 9A; Table 3). Pectoralis EMG amplitude was also a good predictor of muscle shortening velocity (Fig. 9B), leading to a strong positive correlation between muscle force and muscle shortening velocity (r^2=0.92). Because of differences in electrode geometry and recording site among individual animals, EMG amplitude only performed well when compared

Table 3. *Additional multiple regression results for muscle power output against wingbeat duration, muscle force and muscle length change*

	r^2	F	P	N
All individuals across speeds	0.82	47.9	<0.0001*	35
One individual across speeds	0.99	246.2	<0.0001*	7
One individual within 1 m s^{-1}	0.94	344.6	<0.0001*	69
One individual within 7 m s^{-1}	0.88	204.4	<0.0001*	86
One individual within 13 m s^{-1}	0.87	116.6	<0.0001*	57

*Indicates significance at P<0.05 after a Bonferroni multiple test correction for all electromyogram (EMG) regression tests.

as a predictor of muscle force or shortening velocity within an individual over a range of motor performance (Table 4; see Loeb and Gans, 1986). However, despite these difficulties in comparing among individuals, the analyses were still significant. Normalizing both EMG amplitude and muscle force prior to performing the regression tests compensated for some of the differences among individuals, improving the fit of the data (Table 4). Among wingbeats within a given speed, the variation in peak muscle force exceeds that of EMG amplitude, resulting in a weaker relationship between amplitude and force when considering results from a single flight speed (Table 4). This difference in the magnitude of variation between EMG amplitude and force within a speed probably reflects how changes in wing position and the aerodynamic resistance to wing motion affect the peak force developed by the cockatiel pectoralis on a wingbeat-by-wingbeat basis. Finally, we found that the relationship between EMG amplitude and both force and mean shortening velocity during downstroke was not significant among wingbeats at speeds of 11 m s^{-1} and 13 m s^{-1} (Fig. 9).

Discussion

We previously found that muscle power output in cockatiels flying across a range of steady speeds (1–13 m s^{-1}) in a wind tunnel varied 2.2-fold in a U-shaped manner consistent with aerodynamic theory (Tobalske et al., 2003), which is in contrast to the asymmetric L-shaped curve described previously in magpies (Dial et al., 1997). In the present study, we extended these results to examine in-depth the sources of the observed variation in power output. Our analysis shows that cockatiels modulate pectoralis power output primarily by modulating muscle force production.
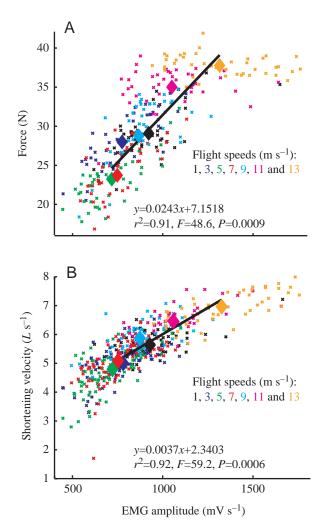

Fig. 9. (A) A least-squares regression of muscle force *versus* electromyogram (EMG) amplitude within one individual across speeds. (B) A least-squares regression of muscle shortening velocity during downstroke *versus* EMG amplitude within the same individual across speeds. EMG amplitude was quantified as the integrated rectified EMG signal, divided by its duration. We performed the regression against mean values for amplitude, force and shortening velocity at each speed to give a balanced data set. However, we plotted all points included in the mean values as small 'x' symbols to show the full range of variation; the mean values used in the regression analyses are shown as large diamonds. Table 4 reports additional analyses of EMG amplitude with respect to muscle force.

Based on the correlation of EMG amplitude with muscle force, the changes in force appear to be due to varying motor unit recruitment, acting in concert with adjustments in wing stroke plane and angle of attack, which modulate the aerodynamic coefficients of the wing (Hedrick et al., 2002). This finding generally supported our hypotheses, but we did not anticipate the degree to which muscle force dominates other factors, such as muscle strain, in modulating muscle power output. In contrast to previous studies that focused on maximal power activities, we found that specific features of the contraction cycle, such as the percentage of the cycle spent shortening, did not strongly influence power output and were not used to modulate power across flight speeds. Additionally, although both birds and fishes must generate power to move through a fluid, the strategies used to modulate power output may differ substantially. Our study of cockatiels suggests that birds modulate work and power mainly *via* force, whereas fishes modulate contraction frequency in addition to the recruitment of additional musculature (Altringham and Ellerby, 1999; Syme and Shadwick, 2002). This difference may well reflect the more distinct red and white fiber types found in fish axial musculature compared with the more homogeneous fiber types within the pectoralis of birds (Rosser and George, 1986).

Despite many differences in the requirements for flight *versus* terrestrial locomotion, our results indicate that flying birds and running animals both modulate muscle force production in relation to changes in speed. In flapping flight, muscle force modulates muscle power output, and therefore speed, and is presumably linked to changes in the metabolic cost of flight with speed. Similarly, in terrestrial animals, muscle force production is an important determinant of the metabolic cost of locomotion and maximum speed (Kram and Taylor, 1990; Taylor, 1985; Weyand et al., 2000). Thus, as an underlying component of muscle work and power, force production plays a central role in determining performance in flight, just as it does in terrestrial locomotion.

Modulation of muscle power via *work, force and strain*

The cockatiels in this study modulated pectoralis power output primarily by altering the amount of mechanical work

Table 4. *EMG regression results, EMG amplitude versus peak muscle force*

	r^2	F	P	N
Individual 1 across speeds	0.80	20.00	=0.0066*	7
Individual 3 across speeds	0.91	48.64	=0.0009*	7
Individuals 1 and 3 across speeds				
Actual amplitude and force	0.72	30.44	<0.0001*	14
Normalized amplitude and force	0.77	39.40	<0.0001*	14
Individual #1 within 7 m s^{-1}	0.69	92.21	<0.0001*	43
Individual #3 within 7 m s^{-1}	0.63	142.83	<0.0001*	86

*Indicates significance at $P<0.05$ after a Bonferroni multiple test correction for all electromyogram (EMG) regression tests.

performed during each wingbeat cycle. Muscle work was, in turn, modulated primarily by the amount of force developed by the pectoralis and secondarily by the magnitude of muscle shortening and changes in work loop shape. Peak muscle force and muscle strain both exhibited minima and maxima at the same speeds as overall muscle power output and also varied over a fairly wide range: 1.7-fold and 1.4-fold, respectively. Whereas the range of variation in muscle strain was similar to that found in a previous study of magpies (1.3-fold; Warrick et al., 2001), the variation in force was much greater than that reported previously across flight modes in pigeons (1.4-fold; Dial and Biewener, 1993) and mallard ducks (1.05-fold; Williamson et al., 2001).

Because peak muscle force varied more than muscle strain, it represented the main influence on muscle work and power output. The observed change in muscle force could have been due to the recruitment of additional muscle fibers and/or a shift in the muscle's force–velocity curve towards a slower strain rate and greater force. However, we found that mean strain rate during shortening increased in a manner similar to peak muscle force (Table 2), suggesting that the higher forces were due to greater motor recruitment. This was supported by the strong correlation of EMG amplitude with peak muscle force (Fig. 9A).

Modulation of power via wingbeat frequency

Our hypothesis that muscle power output would be only slightly affected by changes in wingbeat frequency was supported, as wingbeat frequency had a much smaller effect on power than muscle force or strain (Fig. 8). Although wingbeat frequency and pectoralis power both varied in a curvilinear manner with speed, their respective minima occur at different speeds (5 m s^{-1} *versus* 11 m s^{-1}) and their overall ranges of variation differ substantially (2.1-fold *versus* 1.2-fold), resulting in a low, but significant, correlation between wingbeat frequency and power output. We also found that minimum muscle power output occurred at a speed less than half that of minimum wingbeat frequency. Consequently, our results indicate that minimum wingbeat frequency is not necessarily a good experimental indicator of minimum power speed in avian species, contrary to the suggestion of Pennycuick et al. (1996).

Rather than directly reflecting variation in power output, changes in wingbeat frequency may instead be associated with changes in aerodynamic gait. Two gaits have been recognized: a vortex-ring gait used at slower speeds and a continuous vortex gait used at faster speeds (Rayner, 1993; Spedding, 1986, 1987). The distinguishing feature of the vortex-ring gait is that the upstroke produces no useful aerodynamic force, whereas the upstroke of the continuous-vortex gait actively produces lift (Rayner, 1993). Because downstroke duration of the cockatiel remained constant, all changes in wingbeat frequency with speed were due to changes in upstroke duration, which was significantly greater (lower frequency) at the intermediate flight speeds of 7–11 m s^{-1} (Fisher's PLSD; P<0.0001, d.f.=4; Fig. 5). These speeds correspond to the range over which cockatiels apparently use a continuous vortex gait (Hedrick et al., 2002). Thus, cockatiels prolong the upstroke phase of the wingbeat at speeds at which upstroke is thought to produce useful aerodynamic forces.

Although wingbeat frequency, rather than power output, appears to mediate gait change in cockatiels, this may not be the case in all species. Some species, such as the magpie and members of the Phasianidae, do not appear to change gait with speed (Tobalske, 2000). In these species, wingbeat frequency might share a minimum with power output, as has been assumed (Pennycuick et al., 1996).

Variations in muscle duty factor with speed, gait and power

Previous studies *in vitro* have found that asymmetric sawtooth contraction cycles lead to higher work output than do sinusoidal cycles, when the shortening phase is increased relative to the lengthening phase (Askew and Marsh, 2001). This finding is consistent with previous *in vivo* muscle length change results obtained for magpies (Warrick et al., 2001), mallards (Williamson et al., 2001), pigeons (Biewener et al., 1998) and quail (Askew et al., 2001), in which pectoralis shortening occupies 62–67% of the wingbeat cycle. We expected that cockatiels would also use a muscle duty factor greater than 50% at all flight speeds, especially in very slow and fast flight where power requirements are greatest. This also suggests the possibility that modulation of downstroke duration might be a key means for varying muscle work and power output. However, neither of these expectations was strongly supported. The cockatiels did employ an asymmetric 'sawtooth-like' cycle at all speeds, but muscle duty factor was relatively low (54%) at the fastest and highest power speed. Furthermore, downstroke duration did not change significantly with speed, tightly coupling changes in muscle duty factor to changes in wingbeat frequency. Although this prevented direct incorporation of muscle duty factor into our component model of power output, the influence of wingbeat frequency and, therefore, muscle duty factor on power output was negligible. Changes in muscle duty factor should most influence muscle force development and length change, and hence muscle work, rather than muscle power (Askew and Marsh, 2001). However, again we found no significant relationships between wingbeat frequency and muscle strain, peak force or work (P=0.89, 0.63 and 0.80, respectively). Consequently, cockatiels do not appear to modulate their pectoralis shortening duty cycle in order to modulate muscle work and power output as a function of flight speed. Instead, duty cycle appears to be modulated more by changes in underlying gait kinematics.

Changes in work loop shape across speeds

Due to the differing ranges of variation in muscle strain (1.4-fold) and peak force (1.7-fold), work loop shape did not remain uniform across flight speeds. For example, the work loops in Fig. 3B,C appear quite similar, but the loop in Fig. 3C (13 m s^{-1}) has a 60% greater force and only a 40% greater strain than the loop in Fig. 3B (7 m s^{-1}). However, when work loop shape was quantified as the percentage of the theoretical

maximum area actually occupied by the loop, we found that work loop shape did not change significantly with speed (Table 2). We also found that the work loop 'shape factor' had a negative correlation with muscle strain, indicating that there may well be a trade-off between the muscle's ability to optimize its realized 'work space' (for a given force and strain range) and maximizing muscle strain and total work per cycle (Fig. 8). Changes in work loop shape, however, may be an important modulator of muscle power output in situations where there is a shift from minimal power production to positive power, such as when a terrestrial animal shifts from level to uphill running or accelerates.

Muscle force and aerodynamic coefficients

The peak muscle forces generated by the pectoralis during downstroke should generally correspond in timing and relative magnitude to the peak aerodynamic forces experienced by the wings. These aerodynamic forces are proportional to wing shape and area, but we found that the wing adopts a stereotypic, fully outstretched wing posture during peak muscle force production at all flight speeds. Given the invariance in wing shape and assuming that the position of the center of lift on the wing does not change with flight speed, we are able to use the variation in peak muscle force to estimate the variation in the coefficients of lift and drag across a range of flight speeds. In our previous 3-D kinematic analysis (Hedrick et al., 2002), we found that the mean airflow velocity over the distal portion of the wing increased steadily from 7 m s^{-1} to 14 m s^{-1} when flight speed increased from 1 m s^{-1} to 13 m s^{-1}. Results from the present study show that minimum peak muscle force occurred at 5 m s^{-1}. At this speed, we previously found a mean distal wing flow velocity of 8.3 m s^{-1}. With an increase in flight speed from 5 m s^{-1} to 13 m s^{-1}, therefore, our observed 1.7-fold increase in muscle force corresponds to a 1.9-fold increase in air flow velocity past the wing. Because aerodynamic forces increase with the square of flow velocity, this suggests a 3.7-fold increase in aerodynamic force. Thus, in order to maintain an equal relationship between muscle and aerodynamic forces, the mean coefficients of lift and drag must decrease by 2.2-fold over a speed increase from 5 m s^{-1} to 13 m s^{-1}. With a decrease in flight speed from 5 m s^{-1} to 1 m s^{-1}, we found in the present study that muscle force increases 1.4-fold, whereas our earlier results indicate that the square of flow velocity decreases by a factor of 0.7. This differential indicates that mean lift and drag coefficients probably increase 2-fold as cockatiels reduce their flight speed from 5 m s^{-1} to 1 m s^{-1}. Therefore, our results suggest that changes in wing orientation result in a 4-fold decrease in the coefficients of lift and drag as a cockatiel's flight speed increases from 1 m s^{-1} to 13 m s^{-1}. This range of variation is compatible with recent experimental tests of bird wing lift and drag coefficients in revolution (Usherwood and Ellington, 2002), given the observed range of variation in estimated angle of attack with speed for cockatiels flying in our wind tunnel (37° to 6°; Hedrick et al., 2002).

The 4-fold range of variation in the coefficients of lift and drag predicted for cockatiel wings based on our muscle force results may provide an indirect explanation for why the maximum flight speed of magpies is not limited by muscle power output (Dial et al., 1997). An interesting difference between magpies compared with cockatiels and ringed turtle-doves is that the latter two species generate their respective maximal muscle power outputs at very fast flight speeds, whereas magpies fail to achieve the elevated power outputs at high speeds that they are briefly able to produce when hovering (Tobalske et al., 2003). Consequently, magpies exhibit a rather flat power curve (due to the absence of a significant rise in power at fast speeds), whereas the power curves of cockatiels and ringed turtle-doves are both more acutely concave. Although we have not yet determined coefficients of lift and drag for cockatiel wings, their apparent angles of attack at high speeds are very low, suggesting particularly reduced aerodynamic coefficients (Hedrick et al., 2002). By contrast, magpies have relatively large and broad wings (aspect ratio=5), which may not be capable of being reconfigured to reduce coefficients of drag and lift sufficiently at high flight speeds to avoid a sharp increase in power requirements that might otherwise result.

Flight power modulation across species

The mechanisms used to modulate power output may also scale with body mass. Whereas magpies vary both muscle force and strain similarly to modulate power output (Dial et al., 1997; Warrick et al., 2001), our findings here for cockatiels and our preliminary analysis of ringed turtle-doves (Tobalske et al., 2003) indicate that changes in muscle force are the main means by which these two species vary power output in relation to flight speed. The capacity for enhanced recruitment of muscle force in these smaller species may reflect their ability to elevate power output in fast flight beyond that required at very slow speeds. Earlier studies of pigeons and mallard ducks across a range of flight modes found that pectoralis force also varied only moderately and was not the dominant factor controlling muscle power output. Instead, variation in muscle strain accounted for a majority of the change in power output (Dial and Biewener, 1993; Williamson et al., 2001). Size may be a factor because the two smallest species (cockatiels, 83 g; turtle-doves, 140 g) show the greatest variation in muscle force (1.7-fold and 1.9-fold, respectively), whereas the larger species (pigeons, 649 g; mallards, 995 g) display similar variation in muscle strain (1.3-fold and 1.2-fold, respectively) and force (1.4-fold and 1.1-fold, respectively). Because of their size, larger species in general are believed to have smaller scopes for changing muscle and metabolic power output (Pennycuick, 1968; Ellington, 1991). This is borne out by past metabolic and mechanical power studies of pigeons, which display rather narrow ranges of power output (20–50%; Rothe et al., 1987; Dial and Biewener, 1993). This suggests that, for species in which flight power varies only moderately, both pectoralis force and strain are important to power modulation. In species such as cockatiels, which display a wide range of power outputs, the relative importance of variation in muscle force

via muscle recruitment may be increased due to muscle force–length limitations on the possible range of variation in muscle strain.

Because of the limited sample of *in vivo* flight performance data that is currently available, these interpretations about flight performance, and the possible limits to elevating power output usefully at very fast speeds in larger species or ones with broad, low aspect ratio wings, require additional study. Nevertheless, the underlying mechanisms by which pectoralis contractile function is modulated to vary mechanical, and ultimately aerodynamic power output, are clearly an important determinant of a bird's flight performance range.

Summary

We found that pectoralis contractile function in cockatiels is highly conserved across speed and over a wide range of aerodynamic power requirements. Power output is primarily modulated by muscle force rather than by muscle strain or cycle frequency. Strain rate and EMG results suggest that the additional force is mainly provided *via* increasing pectoralis recruitment rather than by changes in the contractile dynamics – force and length relative to activation phase – of the muscle. Hence, despite the 2-fold range of variation in muscle power output, many aspects of muscle performance vary little. The duration of muscle shortening is invariant, and overall wingbeat frequency and muscle strain vary to a much lesser degree than do muscle power or work. Changes in upstroke duration and, hence, wingbeat frequency may accentuate or facilitate changes in aerodynamic gait: cockatiels appear to use a slow upstroke (continuous vortex gait) at speeds of 7–11 m s^{-1} and a faster upstroke (vortex-ring gait) at other speeds. Due to their effect on the transfer of muscle work into useful aerodynamic work, changes in wing position and orientation during the downstroke probably also affect the magnitude of muscle force developed for a given level of motor recruitment. Analysis of the variation in muscle force and airflow over the wing suggests that lift and drag coefficients probably vary by as much as 4-fold over the speed range examined in this study.

List of symbols

A_0	actuator disc area
a_i	area of a wing strip
$C_{D,par}$	parasite drag coefficient
$C_{D,pro}$	profile drag coefficient
E_p	potential energy
f	wingbeat frequency
F	strain gauge calibration constant
g	gravitational acceleration
H	height of the flight chamber
h	altitude of the bird above the midline of the flight chamber
k_{ind}	induced power correction factor
L	muscle fascicle length
L_0	muscle fascicle resting length
L_{rest}	resting length between sonomicrometry crystals
M_b	body mass
P_{aero}	aerodynamic power
P_{ind}	induced power
P_{par}	parasite power
P_{pro}	profile power
q	dynamic pressure
R	wing length
T	thrust
V_e	equivalent wind speed
V_i	total velocity of a wing strip
V_t	total forward velocity
$\ddot{z}$	vertical acceleration of the bird
Δl	length change
ΔL	total fascicle length change
ε	fascicle strain
ϕ	wing stroke amplitude
θ	angle of the stroke plane relative to vertical
ρ	air density
ρ_0	air density at sea level

References

Altringham, J. D. and Ellerby, D. J. (1999). Fish swimming: patterns in muscle function. *J. Exp. Biol.* **202**, 3397-3403.

Askew, G. N. and Marsh, R. L. (2001). The mechanical power output of the pectoralis muscle of blue-breasted quail (*Coturnix chinensis*): the *in vivo* length cycle and its implications for muscle performance. *J. Exp. Biol.* **204**, 3587-3600.

Askew, G. N., Marsh, R. L. and Ellington, C. P. (2001). The mechanical power output of the flight muscles of blue-breasted quail (*Coturnix chinensis*) during take-off. *J. Exp. Biol.* **204**, 3601-3619.

Barlow, J. B., Rae, W. H., Jr and Pope, A. (1999). *Low-Speed Wind Tunnel Testing*. New York: Wiley-Interscience.

Biewener, A. A., Corning, W. R. and Tobalske, B. W. (1998). *In vivo* pectoralis muscle force–length behavior during level flight in pigeons (*Columba livia*). *J. Exp. Biol.* **201**, 3293-3307.

Biewener, A. A., Dial, K. P. and Goslow, G. E., Jr (1992). Pectoralis muscle force and power output during flight in the starling. *J. Exp. Biol.* **164**, 1-18.

Coughlin, D. J. (2000). Power production during steady swimming in largemouth bass and rainbow trout. *J. Exp. Biol.* **204**, 4249-4257.

Dial, K. P. (1992). Avian forelimb muscles and nonsteady flight: can birds fly without using the muscles of their wings? *Auk* **109**, 874-885.

Dial, K. P. and Biewener, A. A. (1993). Pectoralis muscle force and power output during different modes of flight in pigeons (*Columba livia*). *J. Exp. Biol.* **176**, 31-54.

Dial, K. P., Biewener, A. A., Tobalske, B. W. and Warrick, D. R. (1997). Mechanical power output of bird flight. *Nature* **390**, 67-70.

Durbin, J. (1970). Testing for serial autocorrelation in least squares regression when some of the regressors are lagged dependent variables. *Econometrica* **38**, 410-421.

Ellington, C. P. (1991). Limitations on animal flight performance. *J. Exp. Biol.* **160**, 71-91.

Goldman, D. E. and Heuter, T. F. (1956). Tabular data of the velocity and

absorption of high-frequency sound in mammalian tissues. *J. Acous. Soc. Am.* **28**, 35-37.

Hatze, H. (1988). High-precision three-dimensional photogrammetric calibration and object space reconstruction using a modified DLT-approach. *J. Biomech.* **21**, 533-538.

Hedrick, T. L., Tobalske, B. W. and Biewener, A. A. (2002). Estimates of circulation and gait change based on a three-dimensional kinematic analysis of flight in cockatiels (*Nymphicus hollandicus*) and ringed turtle-doves (*Streptopelia risoria*). *J. Exp. Biol.* **205**, 1389-1409.

Josephson, R. K. (1985). Mechanical power output from striated muscle during cyclical contraction. *J. Exp. Biol.* **114**, 493-512.

Josephson, R. K., Malamud, J. G. and Stokes, D. R. (2000). Power output by an asynchronous flight muscle from a beetle. *J. Exp. Biol.* **203**, 2667-2689.

Kram, R. and Taylor, C. R. (1990). Energetics of running: a new perspective. *Nature* **346**, 265-267.

Loeb, G. E. and Gans, C. (1986). *Electromyography for Experimentalist*s. Chicago: The University of Chicago Press.

McMahon, T. A. (1984). *Muscles, Reflexes, and Locomotion*. Princeton: Princeton University Press.

Norberg, U. M. (1990). *Vertebrate Flight: Mechanics, Physiology, Morphology, Ecology and Evolution*. Berlin: Springer-Verlag.

Pennycuick, C. J. (1968). Power requirements for horizontal flight in the pigeon. *J. Exp. Biol.* **49**, 527-555.

Pennycuick, C. J. (1975). Mechanics of flight. In *Avian Biology*, vol. 5 (ed. D. S. Farner and J. R. King), pp. 1-75. New York: Academic Press.

Pennycuick, C. J., Alerstam, T. and Hedenström, A. (1997). A new low-turbulence wind tunnel for bird flight experiments at Lund University, Sweden. *J. Exp. Biol.* **200**, 1441-1449.

Pennycuick, C. J., Klaassen, M., Kvist, A. and Lindström, Å. (1996). Wingbeat frequency and the body drag anomaly: wind-tunnel observations on a thrush nightingale (*Luscinia luscinia*) and a teal (*Anas crecca*). *J. Exp. Biol.* **199**, 2757-2765.

Rayner, J. M. V. (1979a). A new approach to animal flight mechanics. *J. Exp. Biol.* **117**, 47-77.

Rayner, J. M. V. (1979b). A vortex theory of animal flight. 2. The forward flight of birds. *J. Fluid Mech.* **91**, 731-763.

Rayner, J. M. V. (1993). On the aerodynamics and the energetics of vertebrate flapping flight. *Cont. Math.* **141**, 351-400.

Rayner, J. M. V. (1994). Aerodynamic corrections for the flight of birds and bats in wind tunnels. *J. Zool. Lond.* **234**, 537-563.

Roberts, T. J., Marsh, R. L., Weyand, P. G. and Taylor, C. R. (1997). Muscular force in running turkeys: The economy of minimizing work. *Science* **275**, 1113-1115.

Rosser, B. W. C. and George, J. C. (1986). The avian pectoralis: histochemical characterization and distribution of muscle fiber types. *Can. J. Zool.* **64**, 1174-1185.

Rothe, H.-J., Biesel, W. and Nachtigall, W. (1987). Pigeon flight in a wind tunnel. II. Gas exchange and power requirements. *J. Comp. Physiol. B* **157**, 99-109.

Sokal, R. R. and Rohlf, F. J. (1995). *Biometry*. New York: W. H. Freeman & Co.

Spedding, G. R. (1986). The wake of a jackdaw (*Corvus monedulus*) in slow flight. *J. Exp. Biol.* **125**, 287-307.

Spedding, G. R. (1987). The wake of a kestrel (*Falco tinnunculus*) in flapping flight. *J. Exp. Biol.* **127**, 59-78.

Syme, D. A. and Shadwick, R. E. (2002). Effects of longitudinal body position and swimming speed on mechanical power of deep red muscle from skipjack tuna (*Katsuwonus pelamis*). *J. Exp. Biol.* **205**, 189-200.

Taylor, C. R. (1985). Force development during sustained locomotion: a determinant of gait, speed and metabolic power. *J. Exp. Biol.* **115**, 253-262.

Tobalske, B. W. (1995). Neuromuscular control and kinematics of intermittent flight in the European starling (*Sturnus vulgaris*). *J. Exp. Biol.* **198**, 1259-1273.

Tobalske, B. W. (2000). Biomechanics and physiology of gait selection in flying birds. *Physiol. Biochem. Zool.* **73**, 736-750.

Tobalske, B. W., Hedrick, T. L., Dial, K. P. and Biewener, A. A. (2003). Comparative power curves in bird flight. *Nature* **421,** 363-366.

Tobalske, B. W., Olson, N. E. and Dial, K. P. (1997). Flight style of the black-billed magpie: variation in wing kinematics, neuromuscular control, and muscle composition. *J. Exp. Zool.* **279**, 313-329.

Usherwood, J. R. and Ellington, C. P. (2002). The aerodynamics of revolving wings: II. Propeller force coefficients from mayfly to quail. *J. Exp. Biol.* **205**, 1565-1576.

Vogel, S. (1994). *Life in Moving Fluids*. Princeton: Princeton University Press.

Wakeling, J. M. and Ellington, C. P. (1997). Dragonfly flight. III. Lift and power requirements. *J. Exp. Biol.* **200**, 583-600.

Walker, J. A. (1998). Estimating velocities and accelerations of animal locomotion: a simulation experiment comparing numerical differentiation algorithms. *J. Exp. Biol.* **201**, 981-995.

Warrick, D. R., Tobalske, B. W., Biewener, A. A. and Dial, K. P. (2001). Sonomicrometry and kinematic estimates of the mechanical power of bird flight. *Bull. Mus. Comp. Zool.* **156**, 257-268.

Weyand, P. G., Sternlight, D. B., Bellizi, M. J. and Wright, S. (2000). Faster top running speeds are achieved with greater ground forces not more rapid leg movements. *J. Appl. Phys.* **89**, 1991-1999.

Williamson, M. R., Dial, K. P. and Biewener, A. A. (2001). Pectoralis muscle performance during ascending and slow level flight in mallards (*Anas platyrhynchos*). *J. Exp. Biol.* **204**, 495-507.

Woltring, H. J. (1986). A FORTRAN package for generalized, cross-validatory spline smoothing and differentiation. *Adv. Eng. Software* **8**, 104-113.